



Electrogenerated chemiluminescence of *N,N*-dimethylamino functionalized tetrakis(phenylethynyl)pyrenes



Yeon Ok Lee^a, Tuhin Pradhan^{a,b}, Kihang Choi^{a,b}, Dong Hoon Choi^{a,b}, Jung Hae Lee^{c,*}, Jong Seung Kim^{a,*}

^a Department of Chemistry, Korea University, Seoul 136-701, Republic of Korea

^b Research Institute for Natural Sciences, Korea University, Seoul 136-701, Republic of Korea

^c Korea Research Institute of Standards and Science, Daejeon 305-600, Republic of Korea

ARTICLE INFO

Article history:

Received 23 March 2013

Received in revised form 2 May 2013

Accepted 7 May 2013

Available online 10 May 2013

Keywords:

Tetrakis(phenylethynyl)pyrene

Substitution *N,N*-dimethylamino group

Radical stability

Intramolecular charge transfer (ICT)

ABSTRACT

The synthesis of star-shaped molecules, comprising a pyrene core with tetrakis(phenylethynyl) arms substituted with *N,N*-dimethylamino and propyl groups (**1–5**), is reported. The electrochemical and photophysical properties of **1–5** depend on the number of *N,N*-dimethylamino groups on the tetrakis(phenylethynyl)pyrene framework. In electrogenerated chemiluminescence (ECL) studies, the spectra of **4** and **5** show red-shifts and band broadening; in contrast, **1** exhibits a typical high-intensity pyrene ECL emission. It was confirmed that the ECL spectra arise from the intramolecular charge transfer (ICT) induced by the annihilation of radical ions owing to the presence of a strong donor.

© 2013 Elsevier Ltd. All rights reserved.

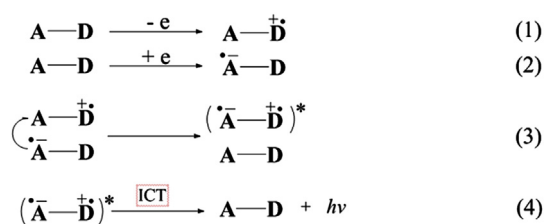
1. Introduction

In electrogenerated chemiluminescence (ECL), a radical species generated at an electrode undergoes a high-energy electron-transfer reaction to form an excited species, which then emits light.¹ The ECL efficiency of luminophores is one of the most important criteria for the evaluating the performance of light-emitting materials.² For the ECL systems of optoelectronic devices, pyrene is a possible radical candidate because of its prominent photophysical properties.³ However, the pyrene molecule has a serious disadvantage as well; the pyrenyl cation radical, which forms in an ECL process, is unstable owing to its intrinsic electron deficiency.⁴

In order to improve the stability of the pyrenyl cation so that they could be used in ECL applications, many pyrene derivatives have been exploited. It has been reported that the ECL efficiency of pyrene is markedly enhanced by increasing π -electron conjugation using specific functional groups on the pyrene framework.^{5–7} Among the various pyrene derivatives, the tetrakis(phenylethynyl)pyrene framework shows high ECL activity because of its considerably developed π -electron networks compared to the mono-, bis-, and tris-substituted pyrene molecules.^{5,7}

However, to date, it has not been determined why the ECL band is affected by changing the functionalization of pyrenes, such as by using electron-donating groups.

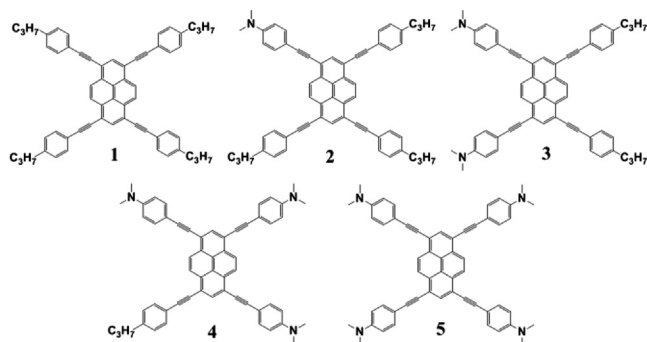
Introduction of certain functional groups to π -conjugation systems can induce different ECL patterns, presumably because their annihilation mechanisms are intrinsically different. In particular, in the presence of strong acceptors or donors in the parent molecule, an excited intramolecular charge transfer (ICT) occurs by the collision of radical anions with radical cations to provide ECL, as seen in Scheme 1.^{8,9} The ICT generally quenches the fluorescence because of a nonradiative pathway; therefore, it could be considered as a factor to change ECL efficiency in optoelectronic materials.^{1b,9}



Scheme 1. ECL emission of donor (D)–acceptor (A)-type luminophores. (1) Radical cation formation. (2) Radical anion formation. (3) ICT formation by direct annihilation. (4) ECL emission.

* Corresponding authors. E-mail addresses: ecljh@kriss.re.kr (J.H. Lee), jongskim@korea.ac.kr (J.S. Kim).

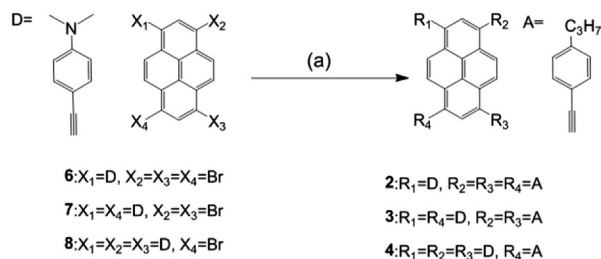
In this study, various electrochemical and photophysical experiments were performed to investigate the possibility that when tetrakis(phenylethynyl)pyrene molecules with different dimethylamino groups (electron donors) are used, the ECL changes so produced are closely related to ICT. This phenomenon has not been exploited before in the ECL studies of the tetrakis-substituted pyrene derivatives. For this purpose, we synthesized tetrakis(phenylethynyl)pyrene derivatives whose structures are depicted in Scheme 2.



Scheme 2. Molecular structures of 1–5.

2. Results and discussion

Pyrene derivatives (2–4) were synthesized by Sonogashira coupling reactions of 6–8 with 4-ethynylpropylbenzene as shown in Scheme 3. Compounds 1, 5, and 6–8 were prepared by adapting the procedures reported earlier.^{5–7}



Scheme 3. Syntheses of 2–4. Reagents and conditions: (a) PdCl₂(PPh₃)₂, CuI, PPh₃, Et₃N, toluene, 100 °C, 3 h.

To gain an insight on the influence of a dimethylamino group on the electrochemical properties of tetrakis(phenylethynyl)pyrene, cyclic voltammetry (CV) was performed using Bu₄NPF₆ in CH₂Cl₂ (0.1 M) with a Pt electrode. These results are summarized in Fig. 1 and Table 1. Each compound, 1–4, showed one reversible reduction peak at –1.93, –1.87, 1.89, and 1.91 V versus SCE, respectively, in contrast, no reverse peak was observed for 5 at 1.91 V. Similar reduction potentials were observed in 1–5, which indicates that the formation of radical anions can be ascribed, not to the nature of the functional groups on the phenyl rings, but to the pyrenyl core.^{5,7}

In contrast, the oxidation peaks of 1–5 showed a trend different from the reduction peaks. First, as the number of donating peripheral substituents increase (from 1 to 5), the compounds are more easily oxidized in the order 0.543 < 0.321 < 0.269 < 0.159 < 0.082 V versus SCE. Second, the reversibility of the oxidation peaks varied on increasing the number of donor atoms. Reversibility in the oxidation peaks was observed for compounds 1, 4, and 5, but not for 2 and 3. These results suggest that electronic communication between the peripheral donor groups and the central acceptors occurs in 2 and 3.

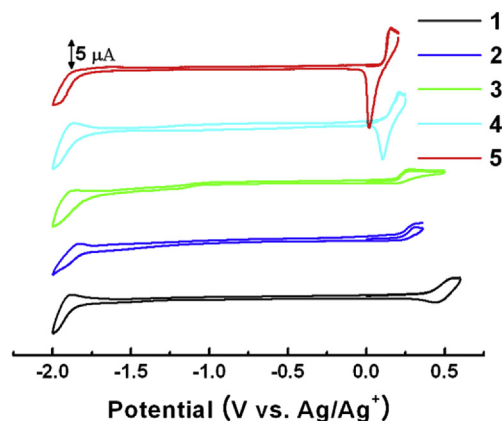


Fig. 1. Cyclic voltammograms of 1–5 (0.5 mM) with a Pt electrode using Bu₄NPF₆ in CH₂Cl₂ (0.1 M). Scan rate=100 mV s⁻¹.

Finally, although the oxidation peaks for 1, 4, and 5 showed good reversibility, the peaks had considerable differences in the current magnitudes. The magnitudes of the anodic peak currents (*i*_{pa} ~ 17 μA and *i*_{pa} ~ 12 μA) for 4 and 5 were three times higher than the anodic current of 1 (*i*_{pa} ~ 4 μA). This implies that with one electron per donor atom, more than three electrons were involved in the oxidation process in 4 and 5. The oxidation and reduction phenomena observed above show that the dimethylamino substituents in a tetrakis(phenylethynyl)pyrene molecule play a crucial role in the redox process, i.e., the cation radical formed by oxidation is very sensitive to the dimethylamino groups. Therefore, it was concluded that in the pyrenyl derivatives, oxidation and reduction take place on the electron-donor atom (A–D^{•+}) and pyrene core (A^{•–}–D), respectively.

Absorption and fluorescence behaviors of all the synthesized compounds were determined in the same solvent used for electrochemistry and ECL experiments and are shown in Fig. 2a and b, respectively. Table 1 summarizes the photophysical parameters of 1–5. As the number of donating peripheral substituents increases, the corresponding wave bands red-shifted. These results are in agreement with a previous report, which states that an electron-donating group allows the HOMO energy level of certain molecules to effectively upshift, causing a red-shift in the absorption spectra.¹¹

Table 1

Parameters obtained from the electrochemical, optical, and theoretical studies for 1–5

Compound	1	2	3	4	5
λ _{abs} ^{max} [nm] ^a	470	473	488	508	509
λ _{em} ^{max} [nm]	494	596	591	603	556
λ _{pa} ^{max} [nm]	612	—	—	633	624
Stokes shift [nm]	24	123	103	123	47
λ _{ECL} ^{max} – λ _{em} ^{max} [nm]	118	—	—	28	68
φ ^b	0.78	0.44	0.22	0.47	0.60
E _{pc} [V]	–1.938	–1.877	–1.899	–1.910	–1.910
E _{pa} [V]	0.543	0.321	0.269	0.159	0.082
ΔE _{gap} ^{elec} [eV] ^c	2.48	2.20	2.17	2.06	1.99
ΔE _{gap} ^{opt} [eV] ^d	2.52	2.36	2.30	2.29	2.27
ΔE _{gap} ^{calc} [eV] ^e	2.50	2.43	2.39	2.37	2.37
HOMO (eV) (calcd)	–4.79	–4.59	–4.43	–4.29	–4.17
LUMO (eV) (calcd)	–2.29	–2.16	–2.04	–1.92	–1.80

^a Recorded at the maximum of the longest spectra in absorption.

^b Using Rhodamine 6G in CH₂Cl₂. φ_r=0.95 in EtOH. Photophysical data was obtained in CH₂Cl₂.¹⁰

^c Electrochemical band gap calculated from the difference between the two redox peak potentials.

^d HOMO–LUMO gap calculated from the lowest-energy UV/vis absorption value in CH₂Cl₂. The photophysical and electrochemical data were obtained in CH₂Cl₂.

^e HOMO–LUMO gap calculated by DFT method at B2LYP/6-31G(d) level of theory.

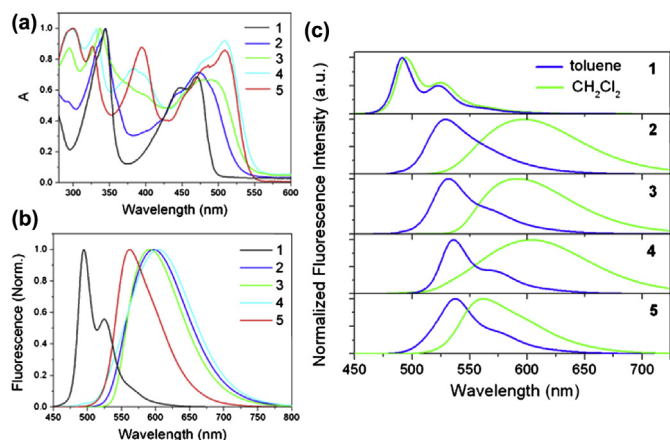


Fig. 2. Steady-state absorption (a) and fluorescence spectra (b) of **1–5** in CH_2Cl_2 . (c) Fluorescence spectra of **1–5** in toluene and CH_2Cl_2 .

Compounds **2–4** exhibited broad emission bands centered at ~ 600 nm, while the maxima of **5** is seen at 556 nm with a narrower band. Compound **1** shows a band at 494 nm with a shoulder peak at 525 nm, which is a typical pyrene emission pattern. A relatively large Stokes shift of 115 nm was observed in **2–4**; in contrast, only a small Stokes shift of 47 nm was seen for **5**. However, the Stokes shift observed in **5** was still greater than that in **1** (24 nm). To gain an insight into this distinctive difference, the emission spectra for all compounds were compared using different solvents (Fig. 2c). In toluene, compounds **2–5** showed almost the same fluorescence patterns as **1**. This reflects that the fluorescence spectra in toluene originate from the Frank–Condon (FC) excited state (or LE state), suggesting negligible CT character. In CH_2Cl_2 (a more polar solvent), the emission bands of **1–5** are different: 494, 596, 591, 603, and 556 nm, respectively. For **2–4**, the fluorescence difference in toluene from CH_2Cl_2 is 64 nm, whereas for **5**, it is only 19 nm, obviously because of **5**'s nonpolar property as verified in previous studies.^{5c} This confirms that in a more polar solvent (CH_2Cl_2), the more developed ICT band gives a larger Stokes shift. Because the degree of ICT character of **2–5** in CH_2Cl_2 is rather weak and revealed moderate fluorescence quantum yields (0.44, 0.22, 0.47, and 0.60, respectively), they should be worthy of application for ECL.

To get insight into the electronic structures, calculation based on density functional theory (DFT) at B3LYP/6-31G(d) level of theory was performed on compounds **1–5**. From the HOMO–LUMO gaps, electrochemical measurements (the difference between oxidation and reduction potentials) and lowest-energy absorption band maxima are listed in Table 1. We noticed that there is a good agreement between computed and experimental results. The HOMO energy increases in going from **1** to **5** (Table 1), which is well correlated with easier oxidation with increasing number of donor groups (**2–5**) as the electrons of donor groups can be released more easily. Frontier molecular orbital surfaces of **1–5** are depicted in Fig. 3. The electron density in HOMOs of **2–5** resides on the pyrene core as well as on the donor arms and electron density delocalization increases with increasing number of donor groups (**2–5**). This overall electron density delocalization in HOMO surfaces could explain the enhanced radical stability in going from **2** to **5**, because upon oxidation the electron-deficient cation radical could be stabilized by other electron-rich donor arms. On the other hand, LUMO is mainly located on pyrene core with some degree of orbital coefficient on triple bond bridges. In this reason, the reduction peaks show little changes among **1–5**. In addition, the intramolecular charge transfer (ICT) from peripheral donor arms to pyrene core occurs.

The ECL spectra of **1–5** (0.5 mM/ CH_2Cl_2) were recorded with 0.1 M Bu_4NPF_6 as a supporting electrolyte (Fig. 4). Compound **1**

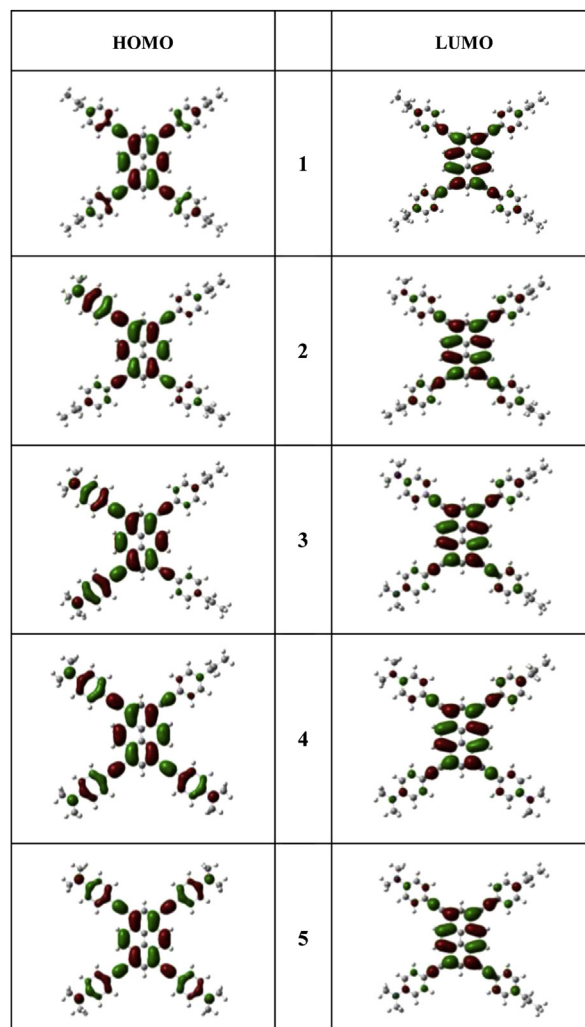


Fig. 3. Profiles of frontier molecular orbitals (highest occupied and lowest unoccupied of **1–5**). Green and red correspond to the different phase of the molecular wave functions for the HOMOs and LUMOs, and the isovalue is 0.02 au.

showed a strong ECL emission at 612 nm because of an excimer band formed by radical ion annihilation, caused by its planar nature.^{1b,7} It was then found that the ECL intensity of **5** at 624 nm is five times smaller than that of **1** and also that **4** shows a much weaker ECL band. However, no ECL activities were observed in **2** or **3**, which is mostly because of instability of the cation radicals. It is notable that the ECL emission of **4** is very weak, despite its electrochemical stability in both oxidation and reduction processes. To understand the quenching behaviors of **4** and **5** in ECL spectra, their fluorescence spectra were compared. The ECL bands of **4** and **5** exhibited red-shifts of 30 and 68 nm, respectively, compared to their fluorescence bands. This undoubtedly implies that the ICT behaviors in **4** and **5** are more developed in electrochemical luminescence than in conventional fluorescence. This is in agreement with the fact that a compound, having both donor and acceptor units and, which shows oxidation and reduction independently in each part, tends to exhibit longer wavelength emission in ECL than in excited state-driven fluorescence, as depicted in Scheme 1.^{1b} As a result, it is concluded that compounds **2** and **3** have an ICT character but negligible ECL intensity because of their radical instability. On the other hand, compounds **4** and **5** reveal more developed ICT as well as stable radical formation for annihilation and give a red-shifted and quenched ECL intensity.

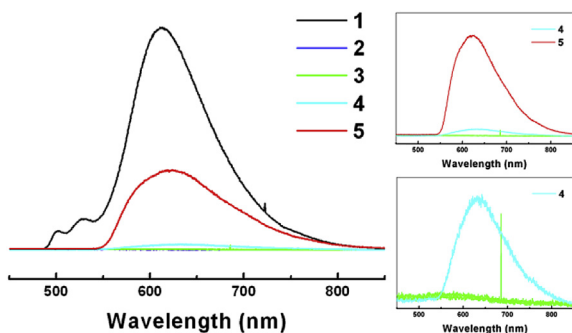


Fig. 4. ECL spectra of 0.5 mM **1–5** with 0.1 M Bu₄NPF₆ in CH₂Cl₂ by pulsing (10 Hz) between peak potentials for reduction and oxidation of the compounds, respectively.

3. Conclusions

In conclusion, a series of tetrakis(phenylethynyl)pyrene derivatives, compounds **1–5**, bearing *N,N*-dimethyl and propyl groups on their *para*-positions were synthesized, and their electrochemical and photophysical properties were determined. In ECL studies, the spectra of **4** and **5** show red-shifts with band broadening while **1** exhibits a typical high-intensity pyrene ECL emission. These ECL spectra arise from the ICT induced by the annihilation of radical ions because of the presence of a strong donor. It was shown that compounds **2** and **3** show a good ICT pattern but negligible ECL intensity, attributed to their radical instability. However, for compounds **4** and **5**, a more developed ICT followed by stable radical formation for annihilation was demonstrated, and hence, a red-shifted and quenched ECL intensity was observed.

4. Experimental section

4.1. Spectroscopic measurements

Absorption spectra were recorded on a Hewlett–Packard 8453 diode array spectrophotometer with 20 μM solution of **1–5** in CH₂Cl₂, while photoluminescence spectra were obtained with a Hitachi F-7000 fluorescence spectrometer with a 1.0-cm standard quartz cell using 3.0 M solutions in various solvents. The fluorescence quantum yields were determined using Rhodamine 6G as the reference using the literature method.¹⁰

4.2. Electrochemistry measurements

CV was carried out using an electrochemical analyzer (CH Instruments 624C). One-Hertz stepwise potentials were generated for 20 s using a CHI 624C. Electrochemical experiments were referenced with respect to the Ag/AgCl reference electrode. All the potentials were measured using ferrocene as an internal standard, where $E_o(\text{Fc}^+/\text{Fc})=70$ mV versus Ag/AgCl. A platinum disk (2 mm diameter) working electrode was polished on felt with 0.05 μM alumina (Buehler), rinsed with water, and sonicated in absolute ethanol for 5 min. Next, it was dried with Ar gas before each experiment. Dichloromethane solutions for CV measurement contained 0.5 mM tetrakis(ethynyl)pyrene and 0.1 M TBAPF₆ as an electrolyte.

4.3. Syntheses

4.3.1. 1-[(4-*N,N*-Dimethylaminophenyl)ethynyl]-3,6,8-tris(4-propylphenylethynyl)pyrene (**2**). Compound **6** (100 mg, 0.172 mmol), PdCl₂(PPh₃)₂ (21 mg, 0.03 mmol), CuI (12 mg, 0.063 mmol), PPh₃ (76 mg, 0.288 mmol), and 1-ethynyl-4-propylbenzene (100 mg, 0.688 mmol) were added to a degassed solution of triethylamine (10 mL) and toluene (50 mL) under Ar. After the mixture was stirred for 3 h at 100 °C, the product was poured into CH₂Cl₂ (200 mL) and

water (200 mL). The organic layer was separated and dried over anhydrous MgSO₄ followed by solvent removal under vacuum. Column chromatography (silica gel, hexane/dichloromethane, 8/2, v/v) gave 45 mg (34%) of an orange red powder. Mp 240–248 °C. IR (KBr pellet, cm⁻¹): 2200 (C≡C), 1594, 1511. ¹H NMR (300 MHz, CD₂Cl₂): δ 8.74 (m, 4H), 8.42 (s, 1H), 8.39 (s, 1H), 7.68 (d, *J*=7.9 Hz, 6H), 7.62 (d, *J*=8.8 Hz, 2H), 7.30 (d, *J*=8.1 Hz, 6H), 6.75 (d, *J*=8.8 Hz, 2H), 3.06 (s, 6H), 2.68 (t, *J*=7.6 Hz, 6H), 1.77–1.65 (m, 6H), 1.00 (t, *J*=7.3 Hz, 9H). ¹³C NMR (100 MHz, CDCl₃): δ 150.5, 143.8, 133.7, 133.2, 132.4, 132.3, 131.9, 128.9, 128.8, 128.7, 127.2, 127.0, 126.7, 126.6, 124.3, 120.7, 120.2, 119.2, 118.9, 97.9, 96.4, 87.6, 86.3, 40.5, 38.3, 24.6, 14.0. MS (FAB) *m/z*: [M]⁺ calcd for C₅₉H₄₉N 771.4; found 771.4.

4.3.2. 1,8-Bis[(4-*N,N*-dimethylaminophenyl)ethynyl]-3,6-bis(4-propylphenylethynyl)pyrene (**3**). Compound **7** (200 mg, 0.56 mmol), PdCl₂(PPh₃)₂ (40 mg, 0.056 mmol), CuI (2.7 mg, 0.056 mmol), PPh₃ (3.7 mg, 0.056 mmol), and 1-ethynyl-4-propylbenzene (242 mg, 1.68 mmol) were added to a gassed solution of triethylamine (50 mL) and toluene (200 mL) under Ar. After stirring for 3 h at 100 °C, the reaction mixture was poured into CH₂Cl₂ (200 mL) and water (200 mL). The organic layer was separated and dried over anhydrous MgSO₄ followed by solvent removal in a vacuum. The crude product was then subjected to column chromatography (silica gel, hexane/dichloromethane, 7/3, v/v) to give 177 mg (41%) of **3** as an orange red powder. Mp 242–260 °C. IR (KBr pellet, cm⁻¹): 2200 (C≡C), 1597, 1511. ¹H NMR (300 MHz, CD₂Cl₂): δ 8.75 (d, *J*=7.5 Hz, 4H), 8.38 (s, 2H), 7.68 (d, *J*=7.9 Hz, 4H), 7.62 (d, *J*=8.9 Hz, 4H), 7.30 (d, *J*=8.0 Hz, 4H), 6.78 (d, *J*=8.8 Hz, 4H), 3.06 (s, 12H), 2.68 (t, *J*=7.73 Hz, 4H), 1.71 (m, 4H), 0.99 (t, *J*=7.4 Hz, 6H). ¹³C NMR (100 MHz, CD₂Cl₂): 150.6, 143.8, 133.3, 133.16, 131.9, 131.5, 128.9, 128.4, 126.9, 126.6, 124.4, 120.7, 119.9, 118.9, 112.1, 110.0, 97.9, 96.2, 87.6, 86.3, 40.4, 38.3, 24.6, 13.9. MS (FAB) *m/z*: [M]⁺ calcd for C₅₈H₄₈N₂ 772.4; found 772.5.

4.3.3. 1,3,6-Tris[(4-*N,N*-dimethylaminophenyl)ethynyl]-8-tris(4-propylphenylethynyl)pyrene (**4**). Compound **8** (300 mg, 0.422 mmol), PdCl₂(PPh₃)₂ (30 mg, 0.042 mmol), CuI (10.5 mg, 0.042 mmol), PPh₃ (11.4 mg, 0.042 mmol), and 1-ethynyl-4-propylbenzene (122 mg, 0.844 mmol) were added to a degassed solution of triethylamine (20 mL) and toluene (100 mL) under Ar. The resulting mixture was stirred at 100 °C for 3 h. The solvent was removed under vacuum to give **4**. The crude product was then subjected to column chromatography (silica gel, hexane/dichloromethane, 6/4, v/v) to yield **4** (137 mg, 42%) as a red powder. Mp 264–276 °C. IR (KBr pellet, cm⁻¹): 2202 (C≡C), 1596, 1513. ¹H NMR (300 MHz, CD₂Cl₂): δ 8.74 (m, 4H), 8.37 (s, 1H), 8.34 (s, 1H), 7.68 (d, *J*=8.2 Hz, 2H), 7.61 (d, *J*=8.9 Hz, 6H), 7.30 (d, *J*=8.0 Hz, 2H), 6.78 (d, *J*=8.9 Hz, 6H), 3.06 (s, 18H), 2.68 (t, *J*=7.6 Hz, 2H), 1.71 (m, 2H), 0.98 (t, *J*=7.3 Hz, 3H). ¹³C NMR (100 MHz, CDCl₃): δ 150.0, 143.7, 133.3, 133.2, 133.1, 132.4, 132.3, 131.9, 128.9, 128.7, 127.0, 126.9, 126.6, 126.4, 127.5, 119.9, 119.6, 118.7, 112.1, 110.3, 97.6, 96.0, 87.8, 86.5, 40.5, 38.3, 24.6, 14.0. MS (FAB) *m/z*: [M]⁺ calcd for C₅₇H₄₇N₃ 773.4, found 773.4.

Acknowledgements

This work was supported by the CRI project (20120000243) (J.S.K.) and Priority Research Centers Program (20120005860) of Research Institute for Natural Sciences from NRF of Korea (K.C. and D.H.C.).

Supplementary data

Supplementary data associated with this article can be found in the online version, at <http://dx.doi.org/10.1016/j.tet.2013.05.010>. These data include MOL files and InChiKeys of the most important compounds described in this article.

References and notes

- (a) Richter, M. M. *Chem. Rev.* **2004**, *104*, 3003; (b) Miao, W. *Chem. Rev.* **2008**, *108*, 2506; (c) Grimsdale, A. C.; Chan, K. L.; Martin, R. E.; Jokisz, P. G.; Holmes, A. B. *Chem. Rev.* **2009**, *109*, 897; (d) Armstrong, N. R.; Wightman, R. M.; Gross, E. M. *Annu. Rev. Phys. Chem.* **2001**, *52*, 391; (e) Fährnich, K. A.; Pravda, M.; Guilbault, G. G. *Talanta* **2001**, *54*, 531.
- (a) Tang, C. W.; VanSlyke, S. A. *Appl. Phys. Lett.* **1987**, *51*, 913; (b) Burroughes, J. H.; Bradley, D. D. C.; Brown, A. R.; Marks, R. N.; Mackay, K.; Friend, R. H.; Burns, P. L.; Homes, A. B. *Nature* **1990**, *347*, 539; (c) Adachi, C.; Baldo, M.; Thompson, M. E.; Forrest, S. R. *J. Appl. Phys.* **2001**, *90*, 5048; (d) Kido, J.; Lizumi, Y. *Appl. Phys. Lett.* **1987**, *73*, 2721; (e) Tessler, N.; Harrison, N.; Friend, R. *Adv. Mater.* **1998**, *10*, 64; (f) Vaeth, R. *Inf. Disp.* **2003**, *19*, 16; (g) Friend, R. H.; Gymer, R. W.; Holmes, A. B.; Burroughes, J. H.; Marks, R. N.; Taliani, C.; Bradley, D. D. C.; DosSantos, D. A.; Bredas, J. L.; Logdlund, M.; Salaneck, W. R. *Nature* **1999**, *397*, 121; (h) Guo, Z.; Song, N. R.; Moon, J. H.; Kim, M.; Jun, E. J.; Choi, J.; Lee, J. Y.; Bielaswki, C. W.; Sessler, J. L.; Yoon, J. *J. Am. Chem. Soc.* **2012**, *134*, 17846; (i) Song, N. R.; Moon, J. H.; Jun, E. J.; Choi, J.; Kim, S.-J.; Lee, J. Y.; Yoon, J. *Chem. Sci.* **2013**, *4*, 1765.
- (a) Figueira-Duarte, T. M.; Müllen, K. *Chem. Rev.* **2011**, *111*, 7260; (b) Antony, J. E. *Angew. Chem., Int. Ed.* **2008**, *46*, 452; (c) Shirota, Y.; Kageyama, H. *Chem. Rev.* **2007**, *107*, 953; (d) Wu, J. S.; Pisula, W.; Müllen, K. *Chem. Rev.* **2007**, *107*, 718.
- Lai, R. Y.; Fleming, J. J.; Merner, B. L.; Vermeji, R. J.; Bodwell, G. J.; Bard, A. J. *J. Phys. Chem. A* **2004**, *108*, 376.
- (a) Oh, J.-W.; Lee, Y. O.; Kim, T. H.; Ko, K. C.; Lee, J. Y.; Kim, H.; Kim, J. S. *Angew. Chem., Int. Ed.* **2009**, *48*, 2522; (b) Kim, H. M.; Lee, Y. O.; Lim, C. S.; Kim, J. S.; Cho, B. R. *J. Org. Chem.* **2008**, *73*, 5127; (c) Sung, J.; Kim, P.; Lee, Y. O.; Kim, J. S.; Kim, D. J. *J. Phys. Chem. Lett.* **2011**, *2*, 818.
- Lee, Y. O.; Pradhan, T.; No, K.; Kim, J. S. *Tetrahedron* **2012**, *68*, 1704.
- Lee, Y. O.; Pradhan, T.; Yoo, S.; Kim, T. H.; Kim, J.; Kim, J. S. *J. Org. Chem.* **2012**, *77*, 11007.
- (a) Lai, R. Y.; Fabrizio, E. F.; Jenekhe, S. A.; Bard, A. J. *J. Am. Chem. Soc.* **2001**, *123*, 9112; (b) Rashidnadimi, S.; Hung, T.-H.; Wong, K.-T.; Bard, A. J. *J. Am. Chem. Soc.* **2008**, *130*, 634.
- (a) Kosower, E. M.; Dodiuk, H.; Kanety, H. *J. Am. Chem. Soc.* **1978**, *100*, 4179; (b) Elangovan, A.; Lin, J.-H.; Yang, S.-W.; Hsu, H.-Y.; Ho, T.-I. *J. Org. Chem.* **2004**, *69*, 8086; (c) Elangovan, A.; Lin, J.-H.; Yang, S.-W.; Hsu, H.-Y.; Ho, T.-I. *J. Org. Chem.* **2005**, *70*, 1104.
- (a) Crosby, G. A.; Demas, J. N. *Phys. Chem.* **1971**, *75*, 991; (b) Yang, W. J.; Kim, C. H.; Jeong, M. Y.; Lee, S. K.; Piao, M. J.; Jeon, S. J.; Cho, B. R. *J. Org. Chem.* **2004**, *16*, 2783.
- (a) Cocchi, C.; Prezzi, D.; Ruini, A.; Caldas, M. J.; Molinari, E. *J. Phys. Chem. Lett.* **2011**, *2*, 1315; (b) Cocchi, C.; Ruini, A.; Prezzi, D.; Caldas, M. J.; Molinari, E. *J. Phys. Chem. C* **2011**, *115*, 2969.